

Constructed Tumor-Targeted and MMP-2 Biocleavable Antibody Conjugated Silica Nanoparticles for Efficient Cancer Therapy

Hao Wu, Xuefeng Ding, Yun Chen, Yanfei Cai, Zhaoqi Yang,* and Jian Jin*

Cite This: *ACS Omega* 2023, 8, 12752–12760

Read Online

ACCESS |



Metrics & More

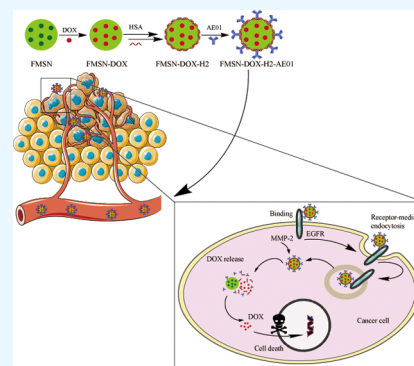


Article Recommendations



Supporting Information

ABSTRACT: Antibody–drug conjugates (ADC) are an inevitable trend in the development of modern “precision medicine”. The goal of this work is to produce enzyme-responsive antibody nanoparticle-loaded medication (FMSN-Dox-H2-AE01) based on the EGFR antibody (AE01) and human serum albumin (HSA) shelled mesoporous silica nanoparticles. HSA and antibodies on the surface of the particles can not only enhance the biocompatibility of the particle and avoid early drug leakage but also allow selective biodegradation triggered by matrix metalloproteinase-2 (MMP-2), which are overexpressed enzymes in some tumor tissues. The cytotoxicity test confirmed favorable safety and efficacy of the ADC. The mortality rate of cancer cells is about 85–90%. Moreover, the antibody nanoparticle-loaded drug showed distinguishing controlled release efficiency toward cancer cells induced by different levels of MMP-2 and pH. This enzyme-responsive FMSN-Dox-H2-AE01 offers a promising option for cancer therapy.



INTRODUCTION

Antibody–drug conjugate (ADC) is to link a biologically active small-molecule drug to a monoclonal antibody by a chemical linker, and the antibody acts as a carrier to target and transport the small-molecule drug to target cells.¹ At present, there are several ADCs already on the market, such as Mylotarg, Kadcyla, Akalux, etc. The successful development of antibody–drug conjugates depend on the suitable selection: (i) target antigen, such as low immunogenicity, high affinity, high specificity, and high internalization rate, etc.;^{2,3} (ii) payload, suitable molecular weight, drug activity, binding site, etc.;⁴ and (iii) linker and linking strategy, suitable drug–antibody ratio (DAR), homogeneity and coupling site, etc.⁵ In recent years, there are two coupling sites for clinical application, namely, the amino (–NH₂) coupling of lysine and the sulfhydryl (–SH) coupling of cysteine. The DAR of the produced ADCs have a significant impact on the drug efficacy and safety.⁶ High DAR often leads to ADCs aggregate and show rapid clearance in vivo, thereby reducing safety and efficacy.^{7,8} Low DAR is problematic in terms of drug efficacy. The optimization of DAR is essential in ADC fabrication.⁹ Drug-loading nanoparticles can deliver large amounts of small molecules without increasing DAR, improving drug efficacy and reducing rapid clearance in vivo.

Mesoporous silica nanoparticle is one of the most commonly used carrier for drug delivery and cancer-targeted therapy, owing to its high accumulation rate at the tumor site resulted from enhanced permeability and retention (EPR) effect.^{10,11} In addition, the large surface area of silica nanoparticles provide sufficient space for different types of functionalization.^{12–14} Therefore, in the current study, fluorescence-doped meso-

porous silicon nanoparticle (FMSN) was adopted as carrier, and the formed AE01-FMSN-Dox-A2 system is expected to take prolonged circulation time to be accumulated at tumor tissues and respond to the enzymatic stimulus to release anticancer drug.

A nanoparticle drug for systemic treatment of solid tumors should generally undergo a five-step [i.e., circulation, accumulation, penetration, internalization, and release (CAPIR)] cascade to transport drugs into cancer cells to exert their therapeutic action. Nanomedicines with a diameter of about 100 nm have longer circulation time and better tumor accumulation effect in the circulation and accumulation process, and nanomedicines with a diameter of <20–30 nm are more conducive to the penetration and diffusion of nanomedicines in dense tumor tissue.^{15,16} Consequently, 100–120 nm nanoparticles were prepared.

Epidermal growth factor receptor (EGFR) is a member of the epidermal growth factor gene (ErbB) family, and 70% of tumor cells have high expression of these receptors, especially nonsmall cell lung cancer, head and neck squamous cell carcinoma, and colorectal cancer, etc.^{17,18} EGFR can activate multiple downstream signal transduction pathways, thereby mediating tumor growth or cancer occurrence,^{17,19} and it is one of the most in-depth and widely concerned tumor

Received: December 14, 2022

Accepted: March 17, 2023

Published: March 29, 2023



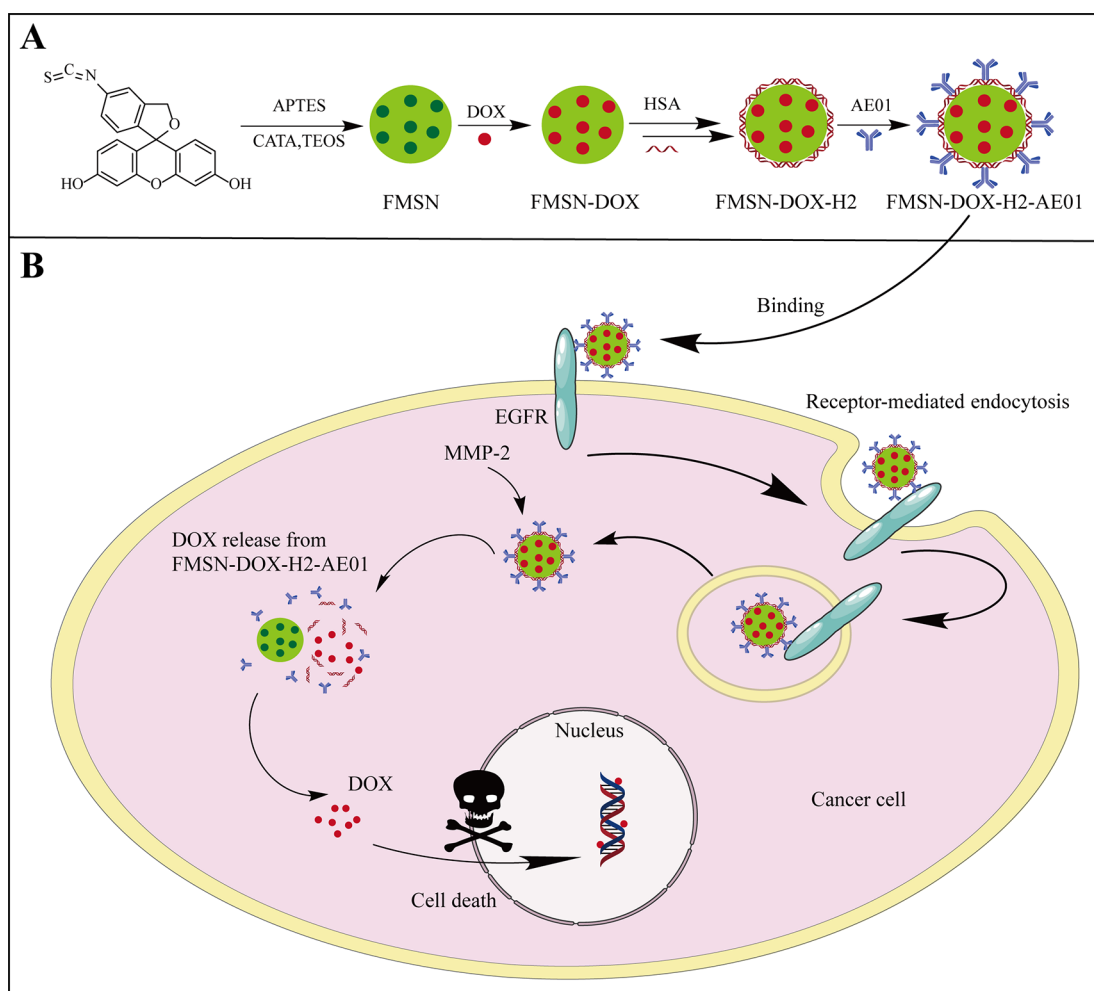


Figure 1. (A) Schematic description of anti-EGFR (AE01) and HSA functionalized mesoporous silica nanoparticles. (B) Mechanism diagram of FMSN-DOX-H2-AE01

therapeutic targets. The high expression of matrix metalloproteinase 2 (MMP-2) can be found in most tumor tissues, such as breast cancer, cervical cancer, ovarian cancer, etc.²⁰ It has been demonstrated that MMP-2 can potentially promote the metastasis of cancer cells, regulate their signal pathways of growth and inhibit tumor apoptosis.²¹ In addition, MMP-2 in the tumor microenvironment is able to biodegrade extracellular matrix (ECM) components, providing more space for cancer cells invasion. These properties have been used to design a number of different enzyme-reactive drug delivery systems.^{22–24} Different from normal cells, the lack of oxygen and the weak acidity of the microenvironment enable it to be a useful biotrigger for controllable and efficient drug delivery system in cancer diagnosis and therapy.²⁵

In this study, we developed an enzyme-responsive antibody nanoparticle-loaded drug based on EGFR antibody (AE01) and HAS shelled mesoporous silica nanoparticles (AE01-FMSN-DOX-A2). Firstly, the antibody AE01 is a new humanized full-length antibody targeting EGFR developed by our team. Second, the blocking HSA of nanoparticles can not only improve the biocompatibility of nanoparticles but also further ensure that cytotoxic drugs will not be released in advance. Moreover, the ratio of drug–antibody (DAR) of nanoparticles could be accurately calculated, which has guiding significance for later clinical experiments. The preparation

process and drug action of FMSN-DOX-H2-AE01 are shown in Figure 1. FMSN-DOX-H2-AE01 is the result of DOX being adsorbed in MSN that has been tagged with FITC, the particle being blocked by HSA and associated with AE01. The early release of DOX is successfully stopped by HSA blockade, which also makes nanoparticles more biocompatible. The transmembrane protein EGFR interacts to FMSN-DOX-H2-AE01 and mediates endocytosis through it. DOX is released through MMP-2 in tumor cells to break down the HSA in the endocytosed FMSN-DOX-H2-AE01. The tumor cells are ultimately killed by the liberated DOX. On the one hand, antibody and HSA are the main biomacromolecules of the native ECM, which can improve the biocompatibility of nanoparticles and prolong blood circulation.^{26,27} On the other hand, AE01 and HAS can plug the pores of nanoparticles and maintain the stability of the drug in blood circulation.^{28,29} In addition, the hollow structure of FMSN allows more small-molecule cytotoxic drug doxorubicin (DOX) to be loaded, thereby increasing the drug–antibody ratio to ensure the killing of tumor cells as much as possible. To verify the above hypothesis, researchers looked at the cytotoxicity of FMSN-DOX-H2-AE01 in both cancer cells and normal cells as well as the drug-releasing impact of MMP-2 and pH values on FMSN-DOX-H2-AE01.

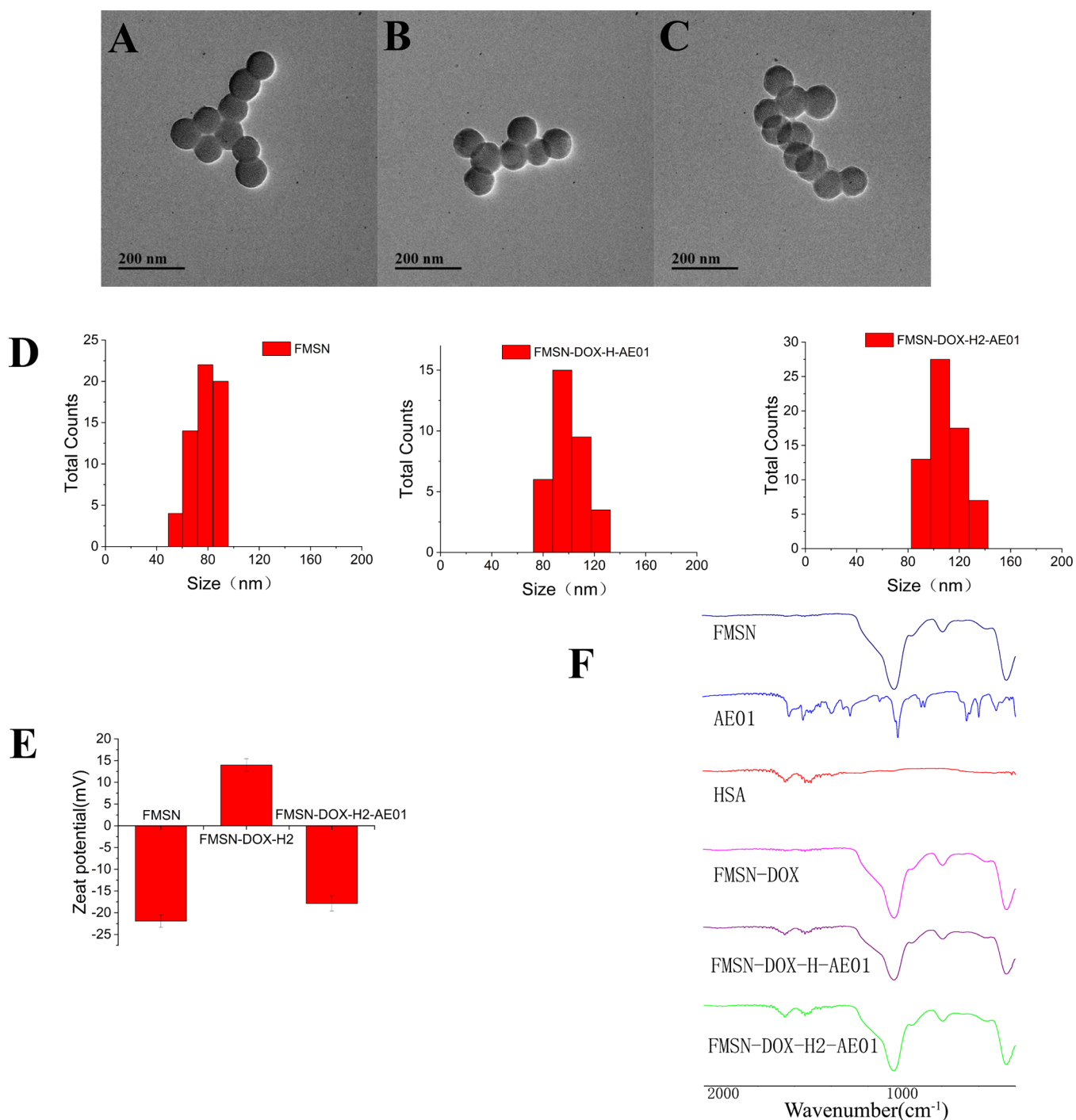


Figure 2. Transmission electronic microscopy images of (A) FMSN-NH₂, (B) FMSN-Dox-H-AE01, and (C) FMSN-Dox-H2-AE01. (D) Dynamic light scattering analysis of FMSN, FMSN-Dox-H-AE01, FMSN-Dox-H2-AE01. (E) Zeta potential of FMSN, FMSN-DOX-H2, FMSN-DOX-H2-AE01. (F) FT-IR images of FMSN, AE01, HSA, FMSN-DOX, FMSN-Dox-H-AE01, FMSN-Dox-H2-AE01.

RESULTS AND DISCUSSION

Characterization of Antibody Nanoparticle-Loaded Drug. The resulting FMSN particles were spherical with uneven surfaces and about 80 nm in diameter (Figure 2A and Figure 2D). FMSN was then aminated, loaded with DOX, and cross-linked with HSA (FMSN-Dox-H). To avoid drug leakage, an additional layer of HSA (FMSN-Dox-H2) was attached. Subsequently, the antibody was covalently anchored to the upper layer of HSA, resulting in the final antibody nanoparticle-loaded drug (FMSN-Dox-H2-AE01). It can be

seen from Figure 2C and Figure 2D that the shape and size of the nanoparticles remains spherical, while the surface tends to be smooth and the size increases to approximate 120 nm in diameter.

The conjugation of AE01 and HSA on particles was estimated qualitatively by zeta potential and FT-IR. As shown in Figure 2E, the zeta potential of FMSN changed from negative to positive after binding to HSA. Once AE01 was anchored, the charge returns to negative again. In the FT-IR image (Figure 2F), the peaks of FMSN-Dox-H2 at 1655

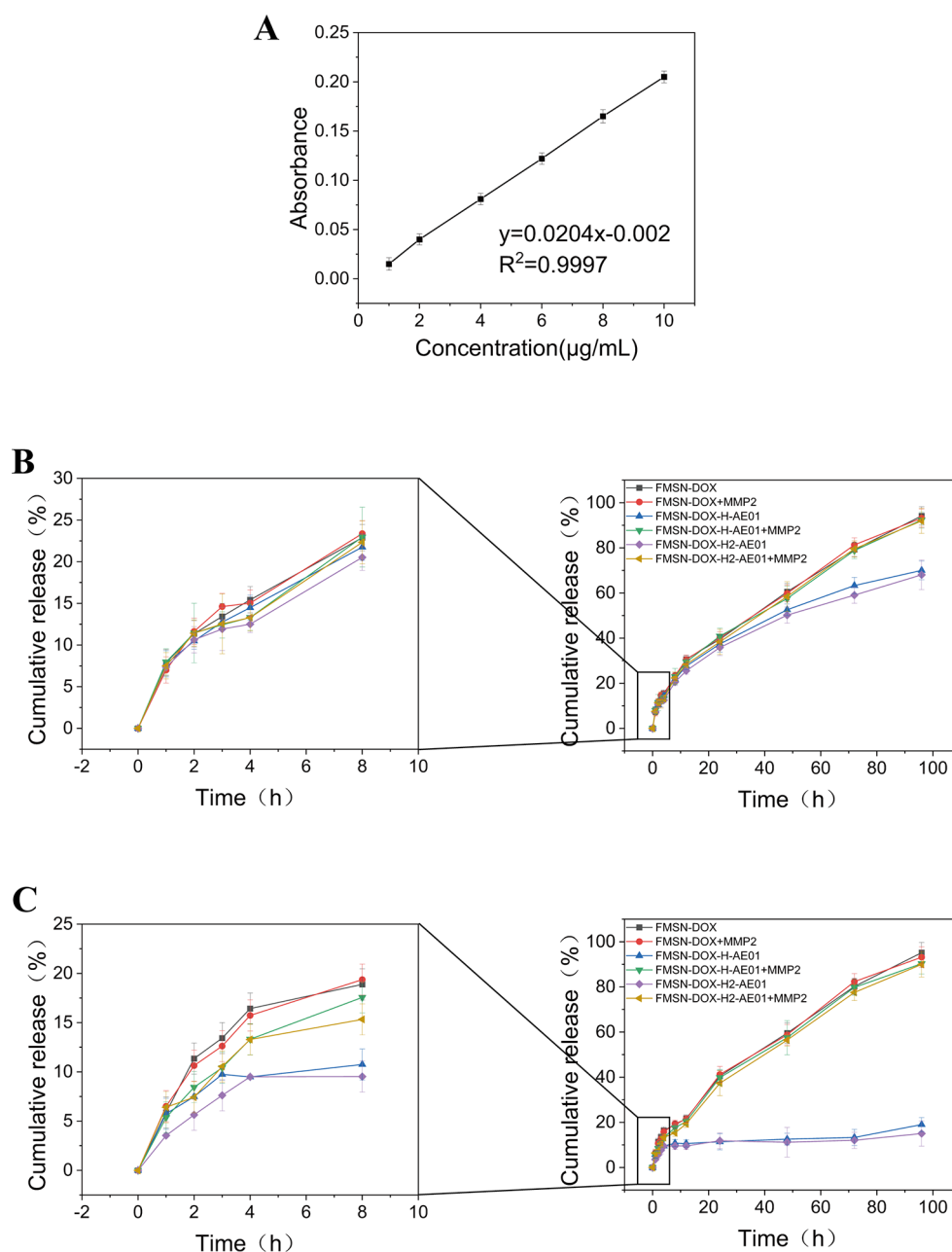


Figure 3. (A) Calibration curve of absorbance at 480 nm vs concentration of Dox in PBS solution. (B) Release profiles of DOX from FMSN-Dox, FMSN-Dox-H-AE01, and FMSN-Dox-H2-AE01 in the absence and presence of MMP-2 (pH 5.6). (C) Release profiles of DOX from FMSN-Dox, FMSN-Dox-H-AE01, and FMSN-Dox-H2-AE01 in the absence and presence of MMP-2 (pH 7.4).

and 1540 cm^{-1} correspond to amide I and amide II bands, respectively, indicating the presence of albumin and antibodies. Nanoparticle tracking analysis (NTA) was performed on FMSN-Dox-H2-AE01 (0.4 mg/mL) suspended in ultrapure water through the NanoSight system. The NTA software tracks the Brownian motion of individual nanoparticles between frames and then calculates the particle concentration to be 7.06×10^7 particles/mL (Figure S2). The obtained results show that FMSN-Dox-H2-AE01 is successfully prepared with a concentration of about 7.06×10^7 particles/mL.

In vitro release of DOX from an Antibody Nanoparticle-Loaded Drug. Before functionalization of HSA and AE01, FMSN was suspended and stirred in DOX solution for drug loading. The amount of DOX encapsulated in the FMSN-

Dox-H2-AE01 was calculated to be 16 mg/g particle based on the UV absorbance at 480 nm of the original drug solution and the collected wash (Figure 3A). Each nanoparticle contains 1.67×10^{-13} mmol DOX can be calculated from the FMSN-DOX-H2-AE01 concentration (eq 1). The molarity of AE01 on each FMSN-DOX-H2-AE01 particle is 1.05×10^{-14} mmol can be calculated (eq 2) depending on the final yield of FMSN-DOX-H2-AE01 of 260 mg and the actual AE01 involved in the reaction of 72.27 mg (see Supporting Information Figure S4). Therefore, the drug–antibody ratio–(DAR) of 15.9 on FMSN-DOX-H2-AE01 particles can be calculated (eq 3).

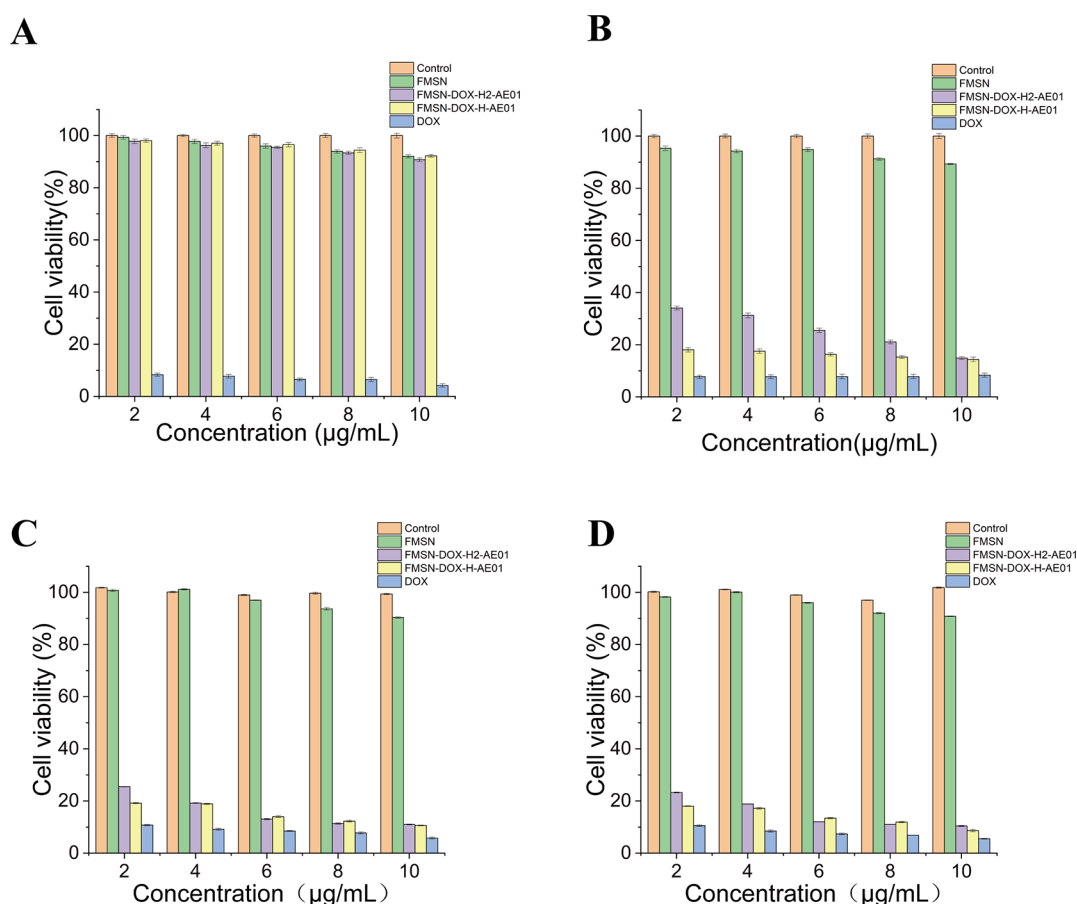


Figure 4. Percent viability of the 293 cells (A), the A431 cells (B), HeLa cells (C), and MCF-7 cells (D) against FMSN, FMSN-Dox-H2-AE01, FMSN-Dox-H-AE01, and DOX in 72 h.

$$\begin{aligned}
 M_{(\text{DOX})\text{ineachFMSN-Dox-H2-AE01}} &= 16/543.52/(7.06 \times 10^7 \times 1000)/0.4 \\
 &= 1.67 \times 10^{-13} \text{ mmol} \quad (1)
 \end{aligned}$$

$$\begin{aligned}
 M_{(\text{AE01})\text{oneachFMSN-Dox-H2-AE01}} &= 72.27/(1.5 \times 10^5)/260 \times 7.06 \times 10^7/0.4 \\
 &= 1.05 \times 10^{-14} \text{ mmol} \quad (2)
 \end{aligned}$$

$$\begin{aligned}
 \text{drug antibody ratio (DAR)} &= 1.67 \times 10^{-13} \text{ mmol} \\
 &/1.05 \times 10^{-14} \text{ mmol} = 15.9 \quad (3)
 \end{aligned}$$

Before and after treatment to MMP-2, the efficacy of DOX release from FMSN-Dox-H2-AE01 and FMSN-Dox-H-AE01 was evaluated at various pH levels. As shown in Figure 3B, when suspended in PBS (pH 5.6) in the absence of MMP-2, the DOX signal increased with time. Within 24 h of adding MMP-2 to this buffer, the DOX signal had risen by around 10–20%. The drug-loaded nanoparticles FMSN-Dox, on the other hand, released DOX both in the presence and absence of the enzyme.

As shown in Figure 3C, no detectable DOX signal was recorded when FMSN-Dox-H2-AE01 and FMSN-Dox-H-AE01 were suspended in PBS buffer (pH 7.4) in the absence of MMP-2, indicating that the particles remained largely intact at this condition. The DOX signal was significantly increased upon addition of MMP-2 to this buffered suspension,

indicating degradation of HSA layers and drug release from the nanoparticles. The release degree of DOX increased to 90% within 96 h. In contrast, the unfunctionalized drug-loaded nanoparticles FMSN-Dox presented DOX release in both the absence and presence of the enzyme. Thus, these results suggest that FMSN-Dox-H2-AE01 and FMSN-Dox-H-AE01 exhibited efficient sealing properties prior to exposure to MMP-2 but specific drug release upon MMP-2 stimulation (pH 7.4). And, as the pH drops as the drug reaches the tumor microenvironment, the drug release effect is further enhanced.

Cytotoxicity of Antibody Nanoparticle-Loaded Drug.

Cytotoxicity test was performed with two different cells, normal cell 293 as the control group and human epidermal squamous carcinoma cells A431, human cervical cancer cells HeLa, and human breast cancer cells MCF-7 as the experimental group. MMP-2 is highly expressed in the A431 cells, HeLa cells, and MCF-7 cells and does not express in the 293 cells.^{20,21,30} The cells were cocultured with different concentrations of FMSN, DOX, FMSN-Dox-H-AE01, and FMSN-Dox-H2-AE01, respectively, and then the cell viability was recorded. When cells were cocultured with FMSN for 72 h, no significant cytotoxicity was observed, and all cell viability remained above 90%. In addition, the cell viability of the 293 cells after coculture with different concentrations of FMSN-Dox-H-AE01 or FMSN-Dox-H2-AE01 for 72 h still remained at high levels because there was no effective MMP-2 in the 293 cells that could degrade HSA and AE01, and the DOX in the nanoparticle pores could not be released (Figure 4A). This result shows that FMSN-Dox-H-AE01 and FMSN-Dox-H2-

AE01 have a good sealing effect in normal cells, reducing the possibility of early drug leakage. However, the cell viability of the A431 cells, HeLa cells, and MCF-7 cells were clearly affected by FMSN-Dox-H-AE01 and FMSN-Dox-H2-AE01. With the increase of drug concentration and coculture time, the viability of cancer cells decreased to about 10–15%, which indicated that MMP-2 degraded the HSA and AE01, released DOX, and thus killed the cancer cells (Figure 4B, 4C, and 4D). The results show that FMSN-DOX-H2-AE01 can effectively kill the three aforementioned tumor cells and be relatively safe to normal cells. This is because AE01 can identify the EGFR that is overexpressed by the tumor cells stated above. The IC_{50} values of the A431 cells, HeLa cells, and MCF-7 cells after 72 h of cocubation with FMSN-Dox-H2-AE01 and FMSN-Dox-H-AE01 were shown in Table 1, and the IC_{50} graph is in Supporting Information (Figure S3).

Table 1. IC_{50} Values of the A431 Cells, HeLa Cells, and MCF-7 Cells ($n = 6$)

	IC_{50} (FMSN-Dox-H2-AE01) ($\mu\text{g}/\text{mL}$)	IC_{50} (FMSN-Dox-H-AE01) ($\mu\text{g}/\text{mL}$)
A431	0.11980	0.08722
HeLa	0.09501	0.03162
MCF-7	0.03103	0.02377

Cellular Uptake of Antibody Nanoparticle-Loaded Drug. To further investigate the efficiency of enzyme responsive and cancer cell targeted drug release, the cellular

uptake performances of FMSN-Dox-H-AE01 and FMSN-Dox-H2-AE01 toward the 293 cells and the A431 cells were reevaluated through flow cytometry; first, FMSN-Dox-H-AE01 and FMSN-Dox-H2-AE01 were cocultured with the cells for 72 h, and the fluorescence intensity of the 293 cells was slightly enhanced (Figure 5A); compared with that of the A431 cells, where the fluorescence intensity was significantly enhanced (Figure 5B). The results showed that the A431 cells took up more nanodrug particles because of the abundant EGFR on the surface of the A431 cells. Next, the intracellular distribution of FMSN-Dox-H2-AE01 in the A431 cells was observed by confocal fluorescence microscopy. FMSN-Dox-H2-AE01 was cocultured with the 293 cells and A431 cells for 72 h. The 293 cells did not show obvious green and red fluorescence (Figure 5C), indicating that the nanoparticles did not enter the 293 cells. The A431 cells showed green and red fluorescence (Figure 5D), indicating that the nanoparticles were endocytosed by the A431 cells. DOX was released into the A431 cells, and also been observed in the nucleus. The above results show that FMSN-Dox-H2-AE01 has stronger binding ability to the A431 cells and can be endocytosed by the A431 cells. Under the action, the HSA and AE01 modified on the surface of the nanoparticles were degraded, so that the DOX in the pores of the nanoparticles is released, resulting in the apoptosis of cancer cells.

The aforementioned findings demonstrate that FMSN-DOX-H2-AE01 can efficiently bind to and be endocytosed by cancer cells that overexpress the EGFR, resulting in the release of DOX and the death of the cancer cells. However, as

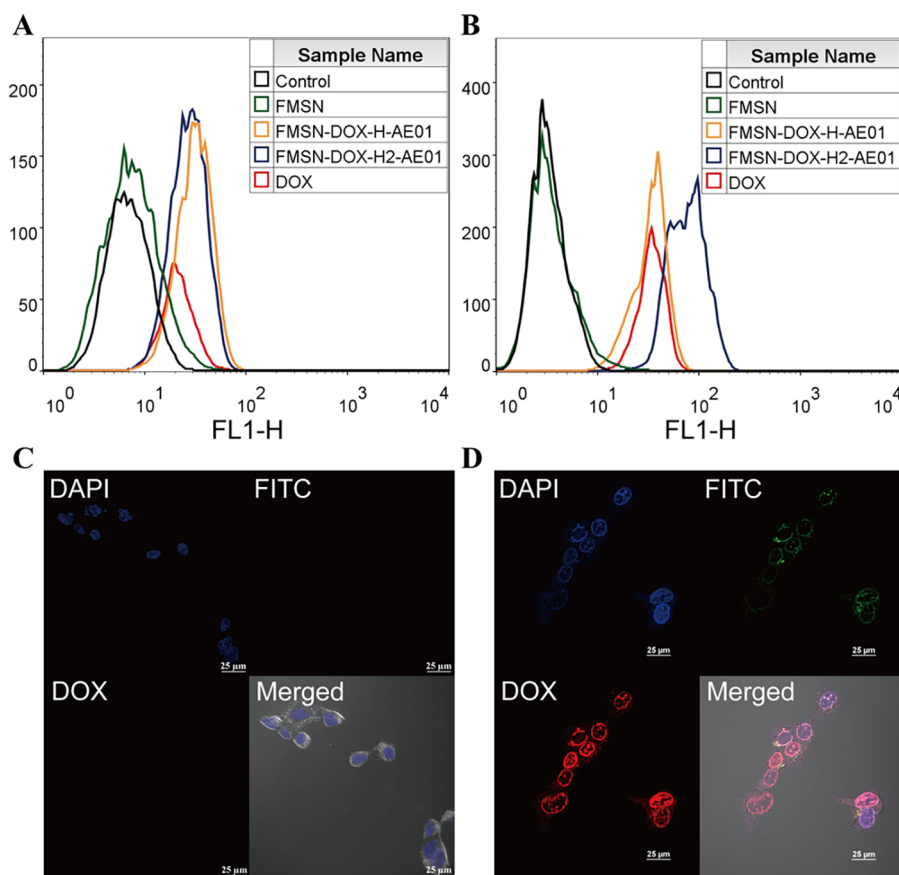


Figure 5. Cellular combinative efficiency of FMSN, DOX, FMSN-Dox-H-AE01, and FMSN-Dox-H2-AE01 in (A) the 293 and (B) A431 cells in 72 h. Confocal laser scanning microscopy (CLSM) images of 10 $\mu\text{g}/\text{mL}$ FMSN-Dox-H2-AE01 in the 293 (C) and A431 cells (D) for 72 h incubation.

normal cells, the 293 cells, do not produce EGFR and FMSN-DOX-H2-AE01 does not attach to them, proving the efficacy and safety of the drug delivery system we developed.

EXPERIMENTAL PROCEDURES

Materials. We prepared a full length humanized EGFR antibody AE01. The VH and VL gene sequences were provided by the laboratory of Professor Cao Boliang of Nanjing Medical University.³¹ The gene sequence and plasmid map of AE01 are shown in [Supporting Information](#). HSA was obtained from previous work of our laboratory.³² (3-Aminopropyl) triethoxysilane (APTES) was from Macklin (Shanghai, PR China). N-hydroxysuccinimide (NHS) was purchased from BBI Life Sciences (Shanghai, PR China). Tetraethyl orthosilicate (TEOS), hexadecyltrimethylammonium chloride (CTAC), methanol, and ethanol were from Sinopharm Biotech (Shanghai, PR China). Fluorescein isothiocyanate (FITC) and 1-(3-dimethylaminopropyl)-3-ethylcarbodiimide hydrochloride (EDC-HCl) were purchased from Aladdin (Shanghai, PR China). Doxorubicin hydrochloride (DOX-HCl) was from Yuancheng (Wuhan, PR China). Matrix metalloproteinases 2 (MMP-2) was purchased from Novoprotein (Shanghai, PR China). The 293 and A431 cells were obtained from the Cell Bank of the Chinese Academy of Sciences (Shanghai, PR China). DAPI Stain Solution and 4% Paraformaldehyde Fix Solution were purchased from Sangon-Biotec (Shanghai, PR China). Dulbecco's modified Eagle's medium (DMEM), fetal bovine serum (FBS), and penicillin–streptomycin solution were purchased from Gibco.

Instruments. Transmission electron microscopy (TEM) images were observed using a JEM-2100 (JEOL, Japan) TEM microscope. FT-IR spectra were measured on a Nicolet TMiSTM 10 (Thermo Fisher Scientific, America). Dynamic light scattering and zeta potential were measured with a ZEN 3600 (Malvern, England) instrument. NanoSight NS300 (Malvern, England) for detection of nanoparticle concentration. UV absorbance spectra were recorded using a UV-2550 (SHIMADZU, Japan) spectrophotometer. Confocal fluorescence images were taken on an TCS SP8 (Leica, German) microscope.

Preparations of FMSN-NH₂. The synthesis and amination of fluorescein isothiocyanate (FITC) labeled mesoporous silica nanoparticles (MSNs) (FMSN) were prepared according to our previous studies.^{33,34} FITC (2.7 mg, 7 μmol) was dissolved in absolute ethanol (1.5 mL) and reacted with aminopropyltriethoxysilane (APTES) (10 μL) for 4 h in the dark to generate FITC-APTES solution. Cetyltrimethylammonium chloride (CTAC) (0.25 g, 0.7 mmol) was dissolved in ultrapure water (120 mL) and NaOH (2 M, 0.75 mL); then, the solution temperature was adjusted to 80 °C and refluxed 30 min to ensure complete dissolution of CTAC. Tetraethyl orthosilicate (TEOS) (1.25 mL) and FITC-APTES solution were added to the solution. The mixture was stirred for an additional 2 h to produce precipitation. The product was obtained by centrifugation and dried under vacuum. To remove CTAC, disperse the coarse particles in acidic methanol (60 mL, 0.6 M HCl) and reflux at 70 °C overnight. FMSN (244 mg) was obtained by repeated template removal until no CTAC signal could be observed by FT-IR and dried under vacuum. For the amination of MSNs, FMSNs were refluxed with 80 mL of toluene containing 0.75 mL of aminopropyltriethoxysilane (APTES) for 4 h and washed 3 times

with 50% ethanol. After drying under vacuum overnight, amino-functionalized MSN (FMSN-NH₂) was obtained.

Preparations of FMSN-Dox-H-AE01. FMSN-NH₂ (500 mg) was dispersed in methanol (100 mL) containing 250 mg of Dox; the mixture was gently stirred at room temperature overnight and distilled under reduced pressure. Repeat the above steps. After drying under vacuum rotary evaporation, ultrapure water (50 mL) was added, and the particles (FMSN-Dox) were obtained by centrifugation. Supernatants were collected to measure drug loading. 100 mg of HSA was dissolved in 100 mL of ultrapure water to maintain pH 5.5, 55 mg of EDC, 32.5 mg of NHS, and FMSN-Dox were added, stirred for 16 h, centrifuged to obtain a precipitate, and washed three times with ultrapure water to obtain FMSN-Dox-H. 100 mg of AE01 was dissolved in 100 mL of ultrapure water, keeping the pH of the solution at 5.5, and after activating the carboxyl group by EDC (55 mg) and NHS (32.5 mg) for 1 h, FMSN-Dox-H was added and stirring was continued for 16 h. The mixture was centrifuged and washed 3 times with ultrapure water. After vacuum drying, FMSN-Dox-H-AE01 was obtained.

Preparations of FMSN-Dox-H2-AE01. FMSN-Dox-A (500 mg) was dispersed in ultrapure water (100 mL) containing 100 mg of HSA, maintained at pH 5.5, and 55 mg of EDC and 32.5 mg of NHS were added; the mixture was stirred for 16 h, centrifuged to obtain the precipitate, and washed with ultrapure water 3 times. After vacuum drying, FMSN-Dox-H2 was obtained. 100 mg of AE01 was dissolved in 100 mL of ultrapure water, keeping the pH of the solution at 5.5, and after activating the carboxyl group by EDC (55 mg) and NHS (32.5 mg) for 1 h, FMSN-Dox-H2 was added and stirring was continued for 16 h. The mixture was centrifuged and washed 3 times with ultrapure water. After vacuum drying, FMSN-Dox-H2-AE01 was obtained.

Drug Release. FMSN-Dox-H2-AE01, FMSN-Dox-H-AE01, and FMSN-Dox particles (2 mg) were dispersed in PBS buffer solution (2 mL, 0.01 M, pH 7.4 or pH 5.6), respectively, and then were sealed in dialysis bags. Immerse the bags in PBS buffer solution (200 mL) and incubate in a shaker at 37 °C, 100 rpm. At predetermined time intervals, remove the PBS medium (3 mL) and perform UV analysis with an absorbance meter. Meanwhile, another 3 mL of fresh PBS was added to the buffer as a supplement. MMP-2 (1 mg/mL, 10 μL) was added to the dialysis bag after shaking for 3 h.

Cytotoxic Studies of FMSN, DOX, FMSN-Dox-H-AE01, FMSN-Dox-H2-AE01. The above compounds were cocultured with the A431, HeLa, MCF-7, and 293 cells in DMEM medium containing 10% FBS and 1% penicillin–streptomycin with 5000 cells/well (100 μL), a temperature of 37 °C, and 5% CO₂; the drug concentration is subject to the content of DOX, ranging from 2 μg/mL to 10 μg/mL. After culturing for 72 h, the medium was removed and MTT was added (100 μL). After four hours, DMSO (100 μL) was added. Finally, cell viability was measured by a Thermo Scientific microplate reader with an emission wavelength of 590 nm.

Analysis of Drug Binding to Cells by Flow Cytometry. The A431 and 293 cells were cultured in DMEM medium containing 10% FBS and 1% penicillin–streptomycin at 37 °C, 5% CO₂. 1 × 10⁵ cells per well were seeded in glass-bottom cell culture dishes and adhered for 24 h. The fresh medium was changed, and then, different concentrations of FMSN-Dox-H2-AE01, FMSN-Dox-H-AE01, and DOX were added. After

incubation for 72 h, the cells were washed with PBS, and then the cell fluorescence was analyzed by flow cytometry.

Cellular Uptake Studies by Confocal Fluorescence Microscopy. The A431 and 293 cells were cultured in DMEM medium containing 10% FBS and 1% penicillin–streptomycin at 37 °C, 5% CO₂. 1 × 10⁴ cells per well were seeded in glass-bottom cell culture dishes and adhered for 24 h. The fresh medium was replaced, and then different concentrations of FMSN-Dox-H2-AE01 were added to incubate the cells for 24 h, 48 h, and 72 h, respectively, and then the cells were washed with PBS and fixed with 4% paraformaldehyde; then, the nuclei were stained with DAPI staining solution, and the cells were washed with PBS and, finally, observed by confocal fluorescence microscopy.

Safety Statements. *Caution!* Corrosive gas HCl gas was purchased only in lecture bottle size. The entire apparatus was setup in a fume hood. Long-gauntlet neoprene gloves and standard lab PPE were work when working on the pressurized system. The sash was always as low as practical for the work.

Statistical Analysis. All the experiments were carried out at least in triplicate, and the results were expressed as mean ± SD. Differences between the control and experimental groups were analyzed by two tailed Student's *t* test. A *P*-value less than 0.05 was considered to be statistically significant.

CONCLUSION

In conclusion, this work described the development of shelled mesoporous silica nanoparticles (FMSN-Dox-H2-AE01) as drug delivery vehicle for tumor therapy. Antibodies on the surface of the particles are able to target the particles for transport to target cells, and HSA has been shown to effectively seal the pores of FMSN, avoiding premature drug leakage. Additionally, the controlled enzyme-responsive release of Dox from the drug delivery system was achieved because of the cleavage of HSA under the degradation of MMP-2. Cytotoxicity, flow cytometry, and confocal assay results demonstrated the cancer cell targeting and normal cell safety of FMSN-Dox-H2-AE01. Therefore, this antibody and HSA multishelled nanoparticle can be a promising candidate as enzyme-responsive ADC for tumor therapy.

ASSOCIATED CONTENT

Supporting Information

The Supporting Information is available free of charge at <https://pubs.acs.org/doi/10.1021/acsomega.2c07949>.

Anti-EGFR DNA and amino acid sequence, design of anti-EGFR double enzyme digestion, schematic diagram of the expression vector, SDS-PAGE, and Western blotting, particle size distribution, concentration, and IC₅₀, and Western blotting of free AE01 in the supernatant of FMSN-DOX-H2-AE01 reaction system (PDF)

AUTHOR INFORMATION

Corresponding Authors

Zhaoqi Yang – School of Life Sciences and Health Engineering, Jiangnan University, Wuxi 214000, People's Republic of China; orcid.org/0000-0002-4485-8872;
Email: Zhaoqiyang@jiangnan.edu.cn

Jian Jin – School of Life Sciences and Health Engineering, Jiangnan University, Wuxi 214000, People's Republic of China; Email: jianjin@jiangnan.edu.cn

Authors

Hao Wu – School of Life Sciences and Health Engineering, Jiangnan University, Wuxi 214000, People's Republic of China; orcid.org/0000-0001-8085-9672

Xuefeng Ding – School of Biotechnology, Jiangnan University, Wuxi 214000, People's Republic of China

Yun Chen – School of Life Sciences and Health Engineering, Jiangnan University, Wuxi 214000, People's Republic of China

Yanfei Cai – School of Life Sciences and Health Engineering, Jiangnan University, Wuxi 214000, People's Republic of China

Complete contact information is available at:

<https://pubs.acs.org/10.1021/acsomega.2c07949>

Notes

The authors declare no competing financial interest.

ACKNOWLEDGMENTS

Thanks to Professor BoliangCao of Nanjing Medical University for providing VH and VL gene sequences. Thanks to Professor Jinghua Chen and Associate Professor Juan Zhou from the School of Life Sciences and Health Engineering, Jiangnan University, for their guidance on this study.

ABBREVIATIONS

ADC, antibody–drug conjugate
HSA, human serum albumin
MMP-2, matrix metalloproteinase-2
DAR, drug–antibody ratio
FMSN, fluorescence-doped mesoporous silicon nanoparticle
EGFR, epidermal growth factor receptor
DOX, doxorubicin

REFERENCES

- (1) Zolot, R. S.; Basu, S.; Million, R. P. Antibody-drug conjugates. *Nat. Rev. Drug Discov* **2013**, *12* (4), 259–60.
- (2) Ritchie, M.; Tchistiakova, L.; Scott, N. Implications of receptor-mediated endocytosis and intracellular trafficking dynamics in the development of antibody drug conjugates. *MAbs* **2013**, *5* (1), 13–21.
- (3) Staudacher, A. H.; Brown, M. P. Antibody drug conjugates and bystander killing: is antigen-dependent internalisation required? *Br. J. Cancer* **2017**, *117* (12), 1736–1742.
- (4) Moldenhauer, G.; Salnikov, A. V.; Luttgau, S.; Herr, I.; Anderl, J.; Faulstich, H. Therapeutic potential of amanitin-conjugated anti-epithelial cell adhesion molecule monoclonal antibody against pancreatic carcinoma. *J. Natl. Cancer Inst* **2012**, *104* (8), 622–34.
- (5) Walter, R. B.; Raden, B. W.; Kamikura, D. M.; Cooper, J. A.; Bernstein, I. D. Influence of CD33 expression levels and ITIM-dependent internalization on gemtuzumab ozogamicin-induced cytotoxicity. *Blood* **2005**, *105* (3), 1295–302.
- (6) Wakankar, A.; Chen, Y.; Gokarn, Y.; Jacobson, F. S. Analytical methods for physicochemical characterization of antibody drug conjugates. *MAbs* **2011**, *3* (2), 161–72.
- (7) Yang, K.; Chen, B.; Gianolio, D. A.; Stefano, J. E.; Busch, M.; Manning, C.; Alving, K.; Gregory, R. C.; Brondyk, W. H.; Miller, R. J.; Dhal, P. K. Convergent synthesis of hydrophilic monomethyl dolastatin 10 based drug linkers for antibody-drug conjugation. *Org. Biomol. Chem.* **2019**, *17* (35), 8115–8124.
- (8) Junutula, J. R.; Flagella, K. M.; Graham, R. A.; Parsons, K. L.; Ha, E.; Raab, H.; Bhakta, S.; Nguyen, T.; Dugger, D. L.; Li, G.; Mai, E.; Lewis Phillips, G. D.; Hiraragi, H.; Fuji, R. N.; Tibbitts, J.; Vandlen, R.; Spencer, S. D.; Scheller, R. H.; Polakis, P.; Sliwkowski, M. X. Engineered thio-trastuzumab-DM1 conjugate with an improved

- therapeutic index to target human epidermal growth factor receptor 2-positive breast cancer. *Clin. Cancer Res.* **2010**, *16* (19), 4769–78.
- (9) Hamblett, K. J.; Senter, P. D.; Chace, D. F.; Sun, M. M. C.; Lenox, J.; Cerveny, C. G.; Kissler, K. M.; Bernhardt, S. X.; Kopcha, A. K.; Zabinski, R. F.; Meyer, D. L.; Francisco, J. A. Effects of Drug Loading on the Antitumor Activity of a Monoclonal Antibody Drug Conjugate. *Clin. Cancer Res.* **2004**, *10* (20), 7063–7070.
- (10) Tang, F.; Li, L.; Chen, D. Mesoporous silica nanoparticles: synthesis, biocompatibility and drug delivery. *Adv. Mater.* **2012**, *24* (12), 1504–34.
- (11) Tarn, D.; Ashley, C. E.; Xue, M.; Carnes, E. C.; Zink, J. I.; Brinker, C. J. Mesoporous silica nanoparticle nanocarriers: bio-functionality and biocompatibility. *Acc. Chem. Res.* **2013**, *46* (3), 792–801.
- (12) Ahmadi, E.; Dehghannejad, N.; Hashemikia, S.; Ghasemnejad, M.; Tabebordbar, H. Synthesis and surface modification of mesoporous silica nanoparticles and its application as carriers for sustained drug delivery. *Drug Deliv* **2014**, *21* (3), 164–72.
- (13) Wang, S.; Liu, F.; Li, X. L. Monitoring of "on-demand" drug release using dual tumor marker mediated DNA-capped versatile mesoporous silica nanoparticles. *Chem. Commun. (Camb)* **2017**, *53* (62), 8755–8758.
- (14) Zhou, J.; Jayawardana, K. W.; Kong, N.; Ren, Y.; Hao, N.; Yan, M.; Ramstrom, O. Trehalose-Conjugated, Photofunctionalized Mesoporous Silica Nanoparticles for Efficient Delivery of Isoniazid into Mycobacteria. *ACS Biomater Sci. Eng.* **2015**, *1* (12), 1250–1255.
- (15) Wang, J.; Mao, W.; Lock, L. L.; Tang, J.; Sui, M.; Sun, W.; Cui, H.; Xu, D.; Shen, Y. The Role of Micelle Size in Tumor Accumulation, Penetration, and Treatment. *ACS Nano* **2015**, *9* (7), 7195–7206.
- (16) Chen, H.; Gu, Z.; An, H.; Chen, C.; Chen, J.; Cui, R.; Chen, S.; Chen, W.; Chen, X.; Chen, X.; Chen, Z.; Ding, B.; Dong, Q.; Fan, Q.; Fu, T.; Hou, D.; Jiang, Q.; Ke, H.; Jiang, X.; Liu, G.; Li, S.; Li, T.; Liu, Z.; Nie, G.; Ovais, M.; Pang, D.; Qiu, N.; Shen, Y.; Tian, H.; Wang, C.; Wang, H.; Wang, Z.; Xu, H.; Xu, J.-F.; Yang, X.; Zhu, S.; Zheng, X.; Zhang, X.; Zhao, Y.; Tan, W.; Zhang, X.; Zhao, Y. Precise nanomedicine for intelligent therapy of cancer. *Science China Chemistry* **2018**, *61* (12), 1503–1552.
- (17) Giaccone, G. EGFR inhibitors in the treatment of lung cancer. *EJC Supplements* **2003**, *1* (5), S106.
- (18) Baselga, J. EGFR therapies in other tumor types. *EJC Supplements* **2003**, *1* (5), S106.
- (19) Maemondo, M.; Inoue, A.; Kobayashi, K.; Sugawara, S.; Oizumi, S.; Isobe, H.; Gemma, A.; Harada, M.; Yoshizawa, H.; Kinoshita, I.; Fujita, Y.; Okinaga, S.; Hirano, H.; Yoshimori, K.; Harada, T.; Ogura, T.; Ando, M.; Miyazawa, H.; Tanaka, T.; Saijo, Y.; Hagiwara, K.; Morita, S.; Nukiwa, T. Gefitinib or Chemotherapy for Non-Small-Cell Lung Cancer with Mutated EGFR. *New England Journal of Medicine* **2010**, *362* (25), 2380–2388.
- (20) Roomi, M. W.; Monterrey, J. C.; Kalinovsky, T.; Rath, M.; Niedzwiecki, A. In vitro modulation of MMP-2 and MMP-9 in human cervical and ovarian cancer cell lines by cytokines, inducers and inhibitors. *Oncol. Rep.* **2010**, *23* (3), 605–614.
- (21) Kessenbrock, K.; Plaks, V.; Werb, Z. Matrix metalloproteinases: regulators of the tumor microenvironment. *Cell* **2010**, *141* (1), 52–67.
- (22) Chen, W. H.; Luo, G. F.; Lei, Q.; Jia, H. Z.; Hong, S.; Wang, Q. R.; Zhuo, R. X.; Zhang, X. Z. MMP-2 responsive polymeric micelles for cancer-targeted intracellular drug delivery. *Chem. Commun. (Camb)* **2015**, *51* (3), 465–8.
- (23) Peng, Z. H.; Kopecek, J. Enhancing Accumulation and Penetration of HPMA Copolymer-Doxorubicin Conjugates in 2D and 3D Prostate Cancer Cells via iRGD Conjugation with an MMP-2 Cleavable Spacer. *J. Am. Chem. Soc.* **2015**, *137* (21), 6726–9.
- (24) Taghizadeh, B.; Taranejoo, S.; Monemian, S. A.; Salehi Moghaddam, Z.; Daliri, K.; Derakhshankhah, H.; Derakhshani, Z. Classification of stimuli-responsive polymers as anticancer drug delivery systems. *Drug Deliv* **2015**, *22* (2), 145–55.
- (25) Ling, D.; Li, H.; Xi, W.; Wang, Z.; Bednarkiewicz, A.; Dibaba, S. T.; Shi, L.; Sun, L. Heterodimers made of metal-organic frameworks and upconversion nanoparticles for bioimaging and pH-responsive dual-drug delivery. *J. Mater. Chem. B* **2020**, *8* (6), 1316–1325.
- (26) Badylak, S. F.; Freytes, D. O.; Gilbert, T. W. Extracellular matrix as a biological scaffold material: Structure and function. *Acta Biomater* **2009**, *5* (1), 1–13.
- (27) Theocharis, A. D.; Skandalis, S. S.; Gialeli, C.; Karamanos, N. K. Extracellular matrix structure. *Adv. Drug Deliv Rev.* **2016**, *97*, 4–27.
- (28) Li, D.; He, J.; Cheng, W.; Wu, Y.; Hu, Z.; Tian, H.; Huang, Y. Redox-responsive nanoreservoirs based on collagen end-capped mesoporous hydroxyapatite nanoparticles for targeted drug delivery. *J. Mater. Chem. B* **2014**, *2* (36), 6089–6096.
- (29) Luo, Z.; Cai, K.; Hu, Y.; Zhao, L.; Liu, P.; Duan, L.; Yang, W. Mesoporous silica nanoparticles end-capped with collagen: redox-responsive nanoreservoirs for targeted drug delivery. *Angew. Chem., Int. Ed. Engl.* **2011**, *50* (3), 640–3.
- (30) Knudson, W.; Bartnik, E.; Knudson, C. B. Assembly of pericellular matrices by COS-7 cells transfected with CD44 lymphocyte-homing receptor genes. *Proceedings of the National Academy of Sciences of the United States of America* **1993**, *90* (9), 4003–4007.
- (31) Wang, X.; Zhu, J.; Zhao, P.; Jiao, Y.; Xu, N.; Grabinski, T.; Liu, C.; Miranti, C. K.; Fu, T.; Cao, B. In vitro efficacy of immunotherapy with anti-EGFR human Fab-Taxol conjugate on A431 epidermoid carcinoma cells. *Cancer Biology & Therapy* **2007**, *6* (6), 980–986.
- (32) Cai, Y.; Chen, Y.; Jin, J. Optimization of biological preparation of human serum albumin. *Journal of Biology* **2020**, *37* (3), 106–109.
- (33) Zhou, J.; Wang, M.; Ying, H.; Su, D.; Zhang, H.; Lu, G.; Chen, J. Extracellular Matrix Component Shelled Nanoparticles as Dual Enzyme-Responsive Drug Delivery Vehicles for Cancer Therapy. *ACS Biomater. Sci. Eng.* **2018**, *4* (7), 2404–2411.
- (34) Lv, X.; Zhang, L.; Xing, F.; Lin, H. Controlled synthesis of monodispersed mesoporous silica nanoparticles: Particle size tuning and formation mechanism investigation. *Microporous Mesoporous Mater.* **2016**, *225*, 238–244.